Pick-up Ion Energization at the Termination Shock

D. Winske, S. P. Gary

Los Alamos National Laboratory

P. Wu and N. A. Schwadron

Department of Astronomy, Boston University

March 9, 2009

Abstract

One-dimensional hybrid simulations are used to investigate how pickup ions are energized at the perpendicular termination shock. Contrary to previous models based on pickup ion energy gain by repeated crossings of the shock front (shock surfing) or due to a reforming shock front, the present simulations show that pickup ion energy gain involves a gyro-phase-dependent interaction with the inhomogeneous motional electric field at the shock. The process operates at all relative concentrations of pickup ion density.

Introduction

The heliospheric termination shock marks the relatively narrow transition between the supersonic outward flow of the solar wind and the slower, deflected flow of the heliosheath. The recent crossings of this shock by Voyager 1 and Voyager 2 [*Richardson et al.,* 2008; *Li et al.,* 2008; *Richardson,* 2008] as well as the October 2008 launch of the IBEX spacecraft with its mission to remotely study the properties of the heliosheath [*McComas et al.,* 2004] have increased interest in the termination shock and its effect on the solar wind plasma. It is generally thought that the termination shock should share many of the properties of other supercritical, quasi-perpendicular space plasma shocks, such as the terrestrial bow shock. It is expected, and V2 observations have confirmed, that the ions should be more strongly heated than the electrons. At the terrestrial bow shock it is well established that ion heating is due to ion reflection [*Sckopke et al.,* 1983]. In this case the reflection is specular; that is, the strong electric and magnetic fields at the shock transition reverse the flow velocity of a small fraction of the upstream ions, which then gain transverse velocity in the motional electric field upstream of the shock, and enter the downstream with substantially enhanced energy. A primary difference between the bow shock and the termination shock is the presence, in the latter case, of a significant component of pickup ions which, by virtue of the pickup process, have a gyrational speed similar to the upstream solar wind flow speed and a corresponding energy of about 1 keV. Voyager 2 crossed the termination shock in August 2007, yielding the first plasma measurements of this structure and, subsequently, of the heliosheath. Initial observations indicated that the shock-heated solar wind ions gained only a small fraction of the energy lost from the decrease in flow speed, so despite the inability of the Voyager 2 instrument to measure the keV ions, *Richardson et al.* (2008) and *Li et al.* (2008) concluded that most of the flow energy of the solar

wind is transferred to the pickup ions. The observed density compression at the shock is about a factor of 2, so that an adiabatic compression of the plasma fluid should yield a temperature increase of the same factor. *Richardson* [2008] infers a downstream pickup ion temperature of 6 to 10 keV; if the upstream pickup gyro-energy is of the order of the solar wind flow energy, these ions are also heated much more than would be predicted by simple fluid compression.

Several simulations, both hybrid [*Liewer et al.,* 1993; *Lipatov and Zank,* 1999] and particle-in-cell [*Chapman et al.*, 2005] have used the two-ion-component scenario to model the termination shock; the interpretation of such computations and associated analytic models have led to two distinct points of view. *Liewer et al*. [1993] concluded that, because the pickup ions have a relatively high speed, they are less subject to reflection than the solar wind ions. They further concluded that solar wind ions are the primary channel for dissipation at the termination shock, although solar wind heating decreases with increasing relative pickup ion density. An opposite viewpoint [*Zank et al.,* 1996] is that the pickup ions are more easily reflected than solar wind ions, and that an appropriate theory of the termination shock may be constructed by ignoring solar wind ion reflection. The hybrid simulations of *Lipatov and Zank* [1999] used finite-mass electrons and very fine spatial resolution to show pickup ion heating by multiple reflected ion acceleration at the perpendicular termination shock (so-called shock surfing [Lee et al., 1996]); their results show support for the *Zank et al*. [1996] analysis. The full particle simulations [*Chapman et al.,* 2005] indicate that the shock periodically reforms; the time-dependent electromagnetic fields lead to energization of the pickup ions.

Recently, *Wu et al*. [2009] executed a series of hybrid simulations of a perpendicular termination shock for a number of different relative pickup ion densities: $0 \le n_{PU}/n_o \le 0.30$. They found that reflection of a fraction of solar wind ions and pickup ion energy gain both contribute

to dissipation at the termination shock. For the parameters of their simulations, *Wu et al*. [2009] found solar wind and pickup ion heating to be equal near $n_{PU}/n_o \sim 0.1$, and that pickup ion heating dominated at larger values of the relative pickup ion density, consistent with the Voyager 2 observations. They also found from analysis of ion trajectories that the concept of specular reflection does not apply to pickup ions, suggesting that a different physical interpretation is needed to describe the energy gain by these more energetic ions.

Results

To simplify the analysis, we consider a perpendicular shock, with upstream flow speed V_0 corresponding to an Alfven Mach number $M_A = V_0/v_A = 8$ and beta of the solar wind, β_{SW}= 0.05, where the Alfven speed v_A and the plasma beta are based on a total upstream proton density n_o and magnetic field B_o. The upstream pickup ions are assumed to have a shell velocity distribution, with $V_{shell} = V_0$. We use a one-dimensional hybrid code, similar to that in *Liewer et al*. [1993] and *Wu et al*. [2009] with a system length in x of 300 c/ω_i (ion inertial lengths based on n_o) and 600 cells; the magnetic field is in the z-direction. The shock is formed by the interaction of the incident solar wind interacting with a hot plasma at the (right) wall. The simulation is run in the downstream plasma frame, so that the incident ions are injected with velocity V_0-V_1 and thus the shock propagates to the left with velocity $-V_1$. Because the shock for weak pickup ion density is rather unsteady for such a low upstream beta, using a relatively coarse resolution (cell size = 0.5 c/ω_i) helps to suppress the unsteadiness [*Hellinger et al*., 2002], which again allows a more transparent picture of how ions are heated at the shock. The electrons are represented as a massless and adiabatic fluid with $\gamma = 5/3$. *Wu et al*. [2009] show that the Rankine-Hugoniot relations are well satisfied across the shock in these simulations when the

compression (heating) factors (γ) for the solar wind and pickup ions are allowed to vary with pickup ion density. We here consider one specific case, with a high number of pickup ions: namely 30% of the upstream total ion density, and for comparison we also briefly discuss the opposing case of 0% pickup ions.

The solid curves in Figure 1 are spatial profiles of the magnetic field, B_z, and the two components of the electric field, E_x and E_y, near the shock after the simulation has run about $\Omega_i t \sim 50$, so that there is a well-formed downstream region. The magnetic field is normalized to its upstream value, and the electric field is normalized to $v_A B_o/c$. One sees in the magnetic field (panel a), the well established characteristics of a supercritical shock: namely a sharp peak (overshoot) of the magnetic field (~ total density since the shock is perpendicular) at the shock front ($x \sim 63$), which is much larger than the average downstream field. In addition, there is an extended rise of the field ("foot") just upstream of the shock front and an increased magnetic field downstream (with compression ratio ~ 2) that shows a number of large, quasi-periodic oscillations. The E_x profile is zero upstream of the shock, shows a decrease in the foot (i.e., an increase in the electrostatic potential, $E_x = -\nabla\varphi$), that slows the upstream flow, and a sharp dip and peak in E_x at the shock front that is due to the fact that $E_x \sim -\nabla p_e \sim -\nabla B_z$. Profiles in E_y show the expected motional electric field upstream of the shock [$E_y = (V_0 - V_1)B_z/c$], which is reduced significantly in the foot. Ey has a large negative spike at the shock front that is due to the large overshoot in B_z, and goes to zero in the downstream, where the flow is essentially zero.

For comparison, we show as dotted lines in Figure 1 the results of a second simulation where the pickup ion fraction is zero. In this case, the shock front is steeper, the overshoot in the magnetic field is larger, the foot is much shorter, the downstream magnetic field is larger, and the downstream oscillations have a much shorter scale length. The changes in E_x and E_y upstream

of the shock scale with the size of the foot and hence also occur on shorter scales. But note that since there is still a large overshoot in the magnetic field, the large negative spike in E_y persists at the shock front. In this case, the shock structure is well known from observations at the bow shock [e.g., *Scudder et al.,* 1986]. The spatial structure is correlated with a fraction of the solar wind ions that are reflected at the shock, which then gain enough energy in the upstream motional electric field to pass into the downstream and contribute dominantly to the downstream heating. Observations at the terrestrial bow shock [*Sckopke et al.,* 1983] and simulations [*Leroy et al.,* 1981] show that the reflection process is nearly specular in the shock frame ($v_x \rightarrow - v_x$, with v_y remaining small) and the slowing down in the foot of the ions that are reflected at the shock involves not only E_x (i.e., the shock potential), but also the contribution from $v_y B_z/c$. The results at high pickup ion fraction thus indicate some type energization involving the pick-up ions that then gives rise to the extended foot and longer spatial scales of the downstream oscillations.

Figure 2 shows additional results of the same simulation (with 30% pickup ions) showing the separate number density and x and y components of the flow velocity of each ion species (normalized to their upstream densities and v_A); the solar wind quantities are plotted as solid lines, the pickup ion quantities as dotted lines. While the density of the solar wind ions shows a large enhancement at the shock transition, an extended foot, and downstream oscillations related to the peaks in B_z, the pickup ion density rises earlier before the shock and *then is essentially flat through the shock front* and into the downstream. The V_x profile shows the pickup ions slow considerably upstream of the shock, while V_y of the pickup ions has a large increase in the upstream region. The solar wind ions are slowed considerably upstream of the shock in the extended foot.

Figure 3 shows the velocity space plots (v_x - v_y) of pickup ions (left panels) and solar wind ions (right panels) [in the simulation = downstream frame] within 20 c/ω_i of the shock front, at the same time as the previous plots. (The velocity distributions farther upstream and downstream from the shock front are shown in *Wu et al.* [2009].) The solar wind ions (panel b) show: (1) a collection of slowed upstream ions with $v_x/v_A \sim$ 1-5, (2) a thermalized downstream population with $v_x \sim 0$ and (3) a component extending with small v_y from the slowed upstream peak to negative velocities ($v_x \sim$ -6). This last component is the solar wind ions that are specularly reflected and then acquire some energy through v_y as they return toward the shock and develop a ring-like character. In contrast, the pickup ions (panel a) show a slowed and slightly heated shell, centered on $v_x/v_A \sim 2$. There is a stream of ions that are pulled out from the ring at one particular gyro-phase angle, where $v_x \sim 10$, $v_y \sim$ - 6. These ions continue to gyrate (clockwise), gaining kinetic energy until v_x reaches a maximum and $v_y \sim 0$. Since the ions gyrate, rather than going directly from + v_x to – v_x with only a small change in v_y [as some solar wind ions in panel (b) do], this process is evidently not specular reflection. In fact, there is no reflection at all, since even partial reflection of pickup ions would manifest itself in a significant decrease in the pickup ion V_x at the shock (or a corresponding increase in the pickup ion density), as is seen in the solar wind ions V_x (Fig. 2b). This phase-dependent energy gain can also be seen in the trajectory plots of pickup ions and solar wind ions in Wu et al. [2009]. The flat profiles of pickup ion density and V_x also suggest that the energy gain occurs in one pass through the shock (recall that in the simulation frame the shock is propagating with $-V_1 \sim -3\ V_A$).

The bottom panels in Figure 3 show results from the corresponding case with 0% pickup ions (dotted curves in Figure 1). In this case, the specular nature of the reflection process of the solar wind ions is quite evident in panel (d), as is the significant increase in energy that such ions

subsequently gain as they gyrate back through the shock. The pickup ions (which are test particles in this case) are shown in Fig. 4(c). It is clear that some pickup ions gain energy at the same gyrophase angle as in the 30% case, indicating that the density of pickup ions does not affect the basic energization process. Moreover, there are also a few pickup ions with $v_y > 0$, $v_x < 0$ at even higher energy; these ions have crossed the shock a second time.

Discussion

To understand the energy gain of the pickup ions shown in Figure 3(a,c) in more detail, we consider the diagram shown in Figure 4. The top part of the figure shows the x-y trajectory of a representative pickup ion which gains substantial energy at the shock. (Recall that the simulations are one-dimensional in that they follow only ion motion in the x-direction, but that the computations follow the full three-dimensional velocities of each macro-particle.) The middle of the figure indicates the spatial variation in E_y at the shock; note that E_y becomes strongly negative at the shock front over a narrow region (the width of the overshoot, $\sim 2\ c/\omega_i$). The bottom of the figure shows the pickup ion motion in v_x - v_y phase space. The dashed circles indicate the gyro-motion in the upstream region. As the motion of this representative pickup ion carries it into the shock (from point A toward point B) (increasing x), its x-velocity decreases, while its y-velocity becomes negative. As the motion of this representative pickup ion carries it into the shock front (point P), E_y is negative, so the ion gains additional v_y negative velocity. As the ion continues to gyrate (from B to C) v_y decreases in magnitude, eventually becoming positive where it gains more energy since E_y is positive. Needless to say, the process of energy gain for a pickup ion is a bit more involved than this, because the electric and magnetic fields are

somewhat spatially varying and there are also contributions from $v_x E_x$. The process is more evident in computer movies of ions at the shock and in the trajectory plots in *Wu et al.* [2009].

The basic picture then is that the pickup ions which gain the most energy at the shock are the fastest ions that have the correct gyro-phase; that is, they encounter the shock from upstream with a large but decreasing v_x and negative but increasing v_y (point P in Figure 4). The gyro-motion of these particles then carries them to an increasingly negative v_y, parallel to the negative E_y in the shock front. Energy gain occurs, since $v_y E_y$ is positive, and thus the electric field does work on these particles. It should be noted that energy gain by $v_y > 0$ with $E_y > 0$ occurs at all shocks when ions reenter the upstream region of the shock (where $E_y > 0$), whether by specular reflection, shock surfing, shock reformation, or wave scattering. *Here, however, the important difference is that the initial kick that pickup ions with large gyro-radii receive occurs at the shock front where $E_y < 0$ and $v_y < 0$.* Note that this picture does not depend on the density of the pickup ions and occurs even for pickup ions as test particles [Fig. 3(c)], as long as there is a negative E_y at the shock (which is always present because of the overshoot in B_z).

The physical picture in Fig. 4 explains why some pickup ions are energized and their gyro-motion carries them back upstream of the shock where they generate an extended foot and longer scale oscillations of B_z and E_y downstream of the shock front (Fig. 1). Such spatial features, of course, are characteristic of shocks with no pickup ions, but the scales of the foot and downstream oscillations are shorter in that case, as the reflected solar wind ions that are responsible have less energy and hence smaller gyro-radii. The phase-dependent energy gain of the pickup ions also gives rise to the large downstream oscillations in V_y, and smaller oscillations in V_x, of the pickup ions in Fig. 2.

It should also be noted that phase space plots of pickup ions in the same format as Figure 3 also appear in *Lipatov and Zank* [1999] and *Chapman et al*. [2005], but look significantly different. In the former case, the simulation involves strong resistive electron heating and very small spatial scales (~ electron Debye lengths), which generates a very large spike in E_x that gives rise to a large acceleration of the pickup ions at the shock. In the later case, the reformation process involves large, time-varying electric fields that likewise can accelerate the pickup ions.

In conclusion, we have presented a new description of pickup ion energy gain at the termination shock through a mechanism that requires ions with a large energy in a shell (or a ring) distribution, i.e., a large gyro-radius with sizeable components of v_x and v_y. These particles sample the region near the shock front, where the motional electric field (E_y) has a large negative spike on the spatial scale of the width of the magnetic field overshoot. This process will also occur if the pickup ion density is small, since there is still an inhomogeneous motional electric field. But it will not occur if the pickup ions are beam-like rather than shell-like (and hence don't have a sizeable v_y velocity component). When the pick-up ions dominate the downstream pressure, the upstream foot and downstream oscillations of B_z have a longer spatial scale length, characterized in terms of the gyro-radius of the energized pickup ions.

Acknowledgments

The authors acknowledge helpful discussions with Gary Zank, Sandra Chapman, and Marty Lee. The Los Alamos portion of this work was performed under the auspices of the U.S. Department of Energy, and was supported by the Solar and Heliospheric Physics SR&T Program of the National Aeronautics and Space Administration.

References

Chapman, S. C., R. E. Lee, and R. O. Dendy (2005), Perpendicular shock reformation and ion acceleration, *Space Sci. Rev., 121,* 5.

Hellinger, P., P. Travnicek and H. Matsumoto (2002), Reformation of perpendicular shocks: Hybrid simulations, *Geophys. Res. Lett.,* 29, 2234.

Lee, M. A., V. D. Shapiro, and R. Z. Sagdeev (1996), Pickup ion energization by shock surfing, *J. Geophys. Res., 101,* 4777.

Leroy, M. M., et al. (1981), Simulation of a perpendicular bow shock, *Geophys. Res. Lett.,* 8, 1269.

Li, H., C. Wang, and J. D. Richardson (2008), Properties of the termination shock observed by Voyager 2, *Geophys. Res. Lett., 35,* L19107, doi:10.1029/2008GL034869.

Liewer, P. C., B. E. Goldstein, and N. Omidi (1993), Hybrid simulations of the effects of interstellar pickup hydrogen on the solar wind termination shock, *J. Geophys. Res., 98,* 15,211.

Lipatov, A. S. and G. P. Zank (1999), Pickup ion acceleration at low -β_p perpendicular shocks, *Phys. Rev. Lett.,* 82, 3609.

McComas, D. J., *et al.* (2004), The Interstellar Boundary Explorer (IBEX), in *Physics of the Outer Heliosphere, 719,* 162, Edited by V. Florinski, N. V. Pogorelov, and G. P. Zank, Am. Inst. of Phys., Melville, NY.

Richardson, J. D. (2008), Plasma temperature distributions in the heliosheath, *Geophys. Res. Lett., 35,* L23104, doi:10.1029/2008GL036168.

Richardson, J. D., J. C. Kasper, C. Wang, J. W. Belcher, and A. J. Lazarus (2008), Cool heliosheath plasma and deceleration of the upstream solar wind at the termination shock, *Nature, 454,* 63.

Sckopke, N., G. Paschmann, S. J. Bame, J. T. Gosling, and C. T. Russell (1983), Evolution of ion distributions across the nearly perpendicular bow shock: Specularly and non-specularly reflected-gyrating ions, *J. Geophys. Res., 88,* 6121.

Scudder, J. D., et al. (1986), The resolved layer of a collisionless, high beta, supercritical, quasiperpendicular shock wave, 2. Dissipative fluid electrodynamics, *J. Geophys. Res.,* 91, 11053.

Wu, P., D. Winske, S. P. Gary, N. A. Schwadron, and M. Lee (2009), Ion heating and energy partition at the heliospheric termination shock, *J. Geophys. Res.,* in prerparation.

Zank, G. P. (1999), Interaction of the solar wind with the local interstellar medium: A theoretical perspective, *Space Sci. Rev., 89,* 413.

Figure Captions

Fig. 1. Profiles across simulated shock: (a) B_z, (b) E_x and (c) E_y versus x for case with 30% pickup ions (solid curves) and 0% pickup ions (dotted curves). B_z normalized to upstream value B_o, E_x and E_z normalized to $B_o v_A/c$, and spatial length x normalized to c/ω_i.

Fig. 2. Profiles of density, x- and y-flow velocities of each ion component (normalized to their upstream densities and v_A) for the 30% pickup ion case; solid curves correspond to solar wind ions, dotted curves to pickup ions.

Fig. 3. Velocity phase space plots (v_x vs v_y) for pickup ions (left panels) and solar wind ions (right panels) within 20 c/ω_i of the shock front: (top panels) case where pickup ion fraction is 0.3; (bottom panels) case where pickup ion fraction is zero. Velocities are normalized by v_A.

Fig. 4. Interpretation of the trajectory of a representative pickup ion which gains energy at the shock [Fig. 3(a)], showing gyro-motion in physical space, spatial profile of E_y and gyro-motion in velocity space.

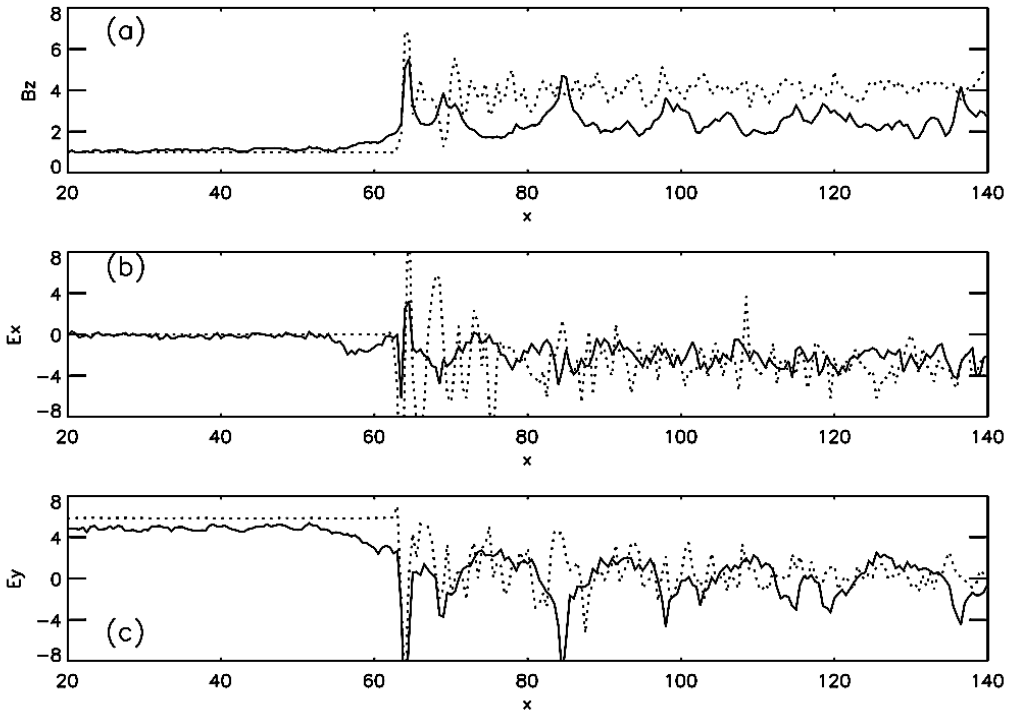

Figure 1

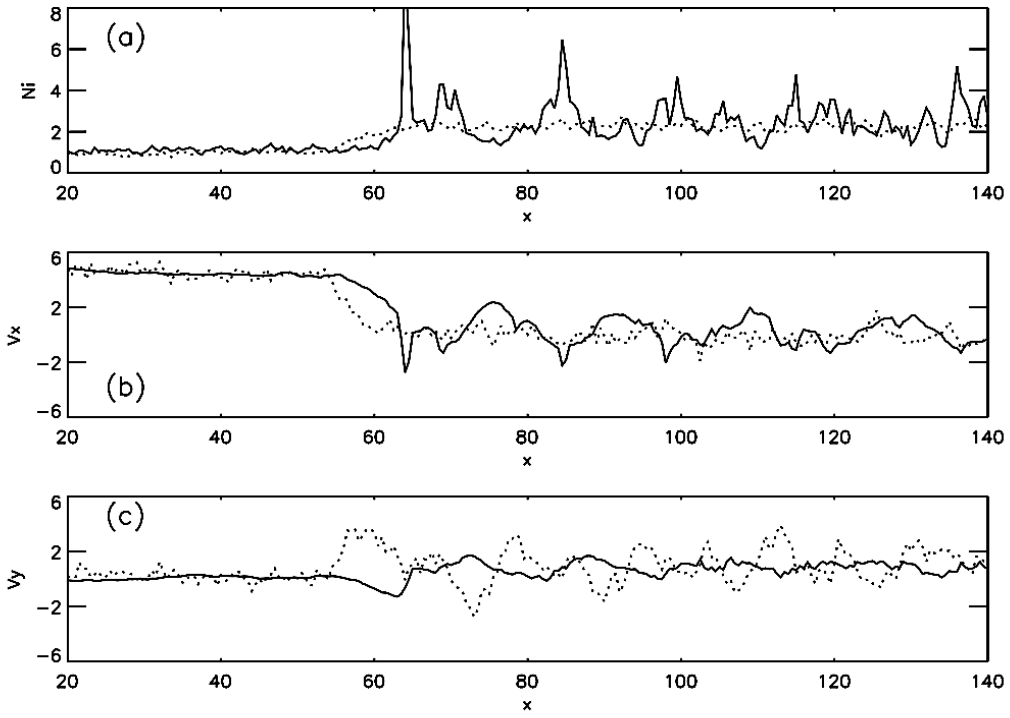

Figure 2

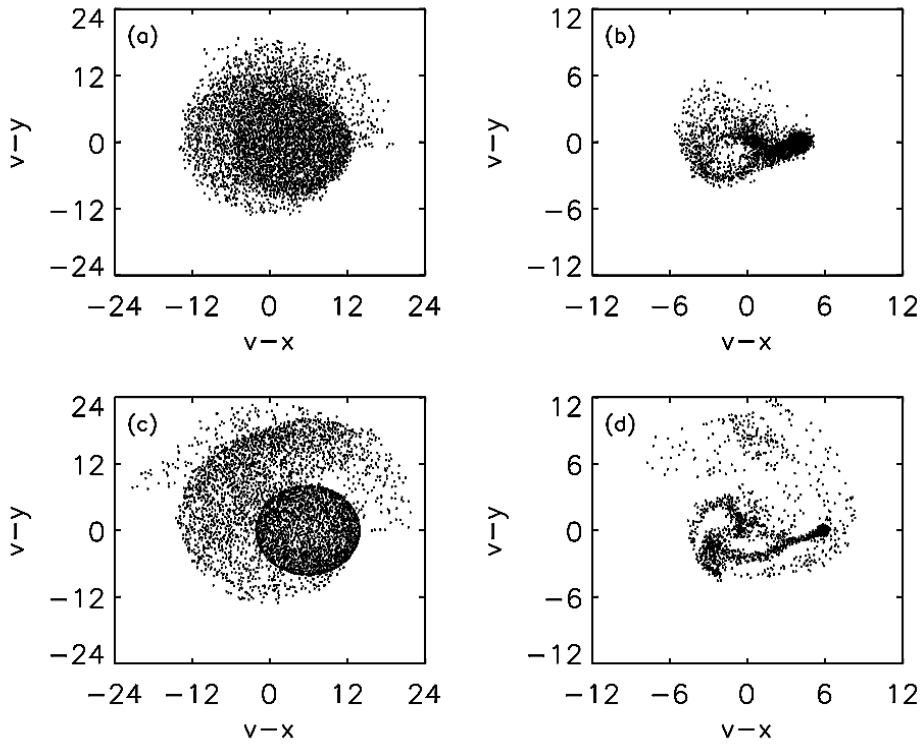

Figure 3

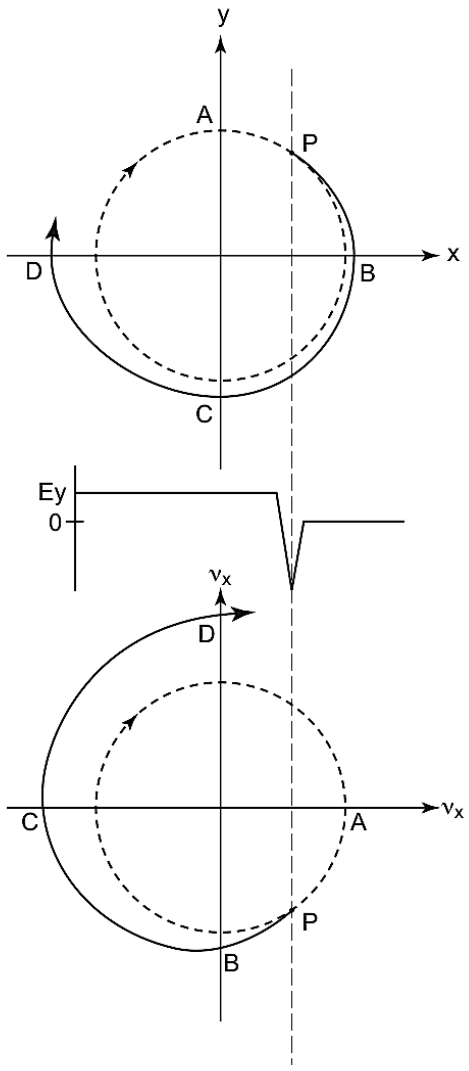

Figure 4